Pergamon

Geochimica et Cosmochimica Acta, Vol. 68, No. 7, p. 1473–1488, 2004

0016-7037/04 $30.00 + .00

doi:10.1016/j.gca.2003.10.003

A conceptual model for near-surface kinetic controls on the trace-element and stable isotope composition of abiogenic calcite crystals

E. Bruce Watson*

Department of Earth and Environmental Sciences, Rensselaer Polytechnic Institute, Troy, NY 12180, USA

(*Received December* 16, 2002; *accepted in revised form October* 6, 2003)

Abstract—The surface of a crystal in equilibrium with solute-bearing fluid generally has a composition that differs from that of the bulk crystal. If the crystal is growing, the surface composition may be "captured" by the newly formed lattice to a degree that depends upon the growth rate and the mobility of atoms in the near-surface region: rapid growth promotes this growth "entrapment," high near-surface mobility works against it. Natural calcites may be particularly susceptible to this kind of kinetic disequilibrium, because their precipitation rates from aqueous solution can be relatively high even at near-ambient temperatures, where ion mobility in the critical near-surface region may be limited.

Existing laboratory data on trace-element uptake as a function of calcite growth rate are examined here in the context of recent discoveries concerning the structure, chemistry and kinetics of the near-surface region of calcite crystals. Recent demonstrations that ions can be mobile in the outermost few nanometers of the calcite lattice even at room temperature have the greatest potential to affect growth entrapment. The model of Watson and Liang (1995)—which quantifies entrapment efficiency in terms of growth rate, diffusivity and surface-layer thickness—is modified to include a depth-dependent diffusivity and possible depletion (as well as enrichment) of some elements in the near-surface region. With these changes, the model is shown to be qualitatively consistent with the body of experimental data on trace element uptake during calcite precipitation.

This apparent success of the model invites application to stable isotopes. Constraining data are few, but available information on oxygen isotope fractionation can be used to show that growth entrapment at ambient temperatures may (depending on model assumptions) produce deviations from calcite/H_2O equilibrium of up to several ‰. The preferred choice of $^{18}O/^{16}O$ for the surface layer is lighter than the lattice equilibrium value, and leads to a reduction in $^{18}O/^{16}O$ of crystals grown at higher growth rates, mimicking "vital effects." *Copyright © 2004 Elsevier Ltd*

1. INTRODUCTION

Several lines of evidence point to a probable role of the calcite/fluid interface in determining the composition of crystals grown inorganically at low temperatures. The evidence includes: 1) preferential bonding of certain trace elements on specific crystallographic surfaces in contact with water (e.g., Paquette and Reeder, 1995; Reeder, 1996); 2) growth-rate dependence of trace-element uptake in controlled laboratory experiments (Lorens, 1981; Davis et al., 1987; Dromgoole and Walter, 1990; Tesoriero and Pankow, 1996); and 3) sector zoning in both natural and synthetic crystals (the cause of which is widely attributed to surface adsorption phenomena; e.g., Reeder and Paquette, 1989).

The above observations appear to be broadly consistent with a general, phenomenological model describing the consequences of surface enrichment to trace-element uptake during crystal growth (Watson and Liang, 1995; Watson, 1996). The main implication of the model is that the concentration of a particular trace-element in a crystal is determined by two things: the concentration of that element in the near-surface region of the crystal (which may be different from that in the bulk lattice) and the outcome of the competition between crystal growth (which can "trap" surface-enriched elements in the crystal lattice) and ion migration in the near-surface region (which attempts to rid the lattice of "unwanted" impurities). In simple terms: *a growing crystal assumes the composition of its surface unless diffusion in the near-surface region is effective during growth*. Because the equilibrium composition of a crystal surface is not necessarily the same as that of the bulk lattice, this statement amounts to a prediction that deviations from thermodynamic partitioning equilibrium can be expected when growth occurs at temperatures where mobility of ions in the near-surface region is limited. It also implies that the magnitude of these deviations could depend systematically upon temperature through the temperature dependence of the diffusivity, growth rate, or surface composition. Kinetic effects that mimic expected dependencies of bulk equilibrium partitioning behavior thus seem possible. Because the concept of partitioning equilibrium applies to isotopes as well as trace elements, all the above "predictions" may also be relevant to fractionation of stable isotopes between crystals and their growth media.

The widespread use of trace-element and stable-isotope characteristics of carbonate minerals to deduce seawater temperature provides ample motivation to revisit the surface-enrichment model at this juncture, with a specific focus upon calcite. Following a brief review of the "growth entrapment" model, two objectives are pursued in the present paper: 1) the viability of an updated version of the model is tested against published

* Author to whom correspondence should be addressed (watsoe@rpi.edu).

results on the growth-rate dependence of trace-element uptake in calcite; and 2) the possible implications of the model for the behavior of oxygen isotopes in the calcite/water system at near-ambient temperatures are discussed.

2. THE "GROWTH ENTRAPMENT" MODEL

2.1. Overview and History

The growth-entrapment model was first described by Watson and Liang (1995) in the context of sector zoning of igneous and metamorphic minerals whose growth rates were arguably very low (e.g., zircon, titanite, staurolite). The model was developed in an effort to explain the seemingly paradoxical observation that sectoral enrichment in minerals—due, presumably, to preservation of anomalous surface composition—can arise even when the crystal growth rate is too low to create a diffusive boundary layer in the contacting growth medium or to preclude equilibrium between the immediate surface and the growth medium. The fundamental premise of Watson and Liang (1995) is that there exists a regime where it is diffusion in the growing crystal, not in the growth medium, that determines the extent to which the crystal lattice can achieve partitioning equilibrium with the growth medium. Thus, if a trace element is selectively enriched on a specific growth surface, and if the diffusivity of that element in the near-surface region of the crystal is low, then the anomalous surface composition may be partially or completely preserved within the growth sector formed behind that surface.

Watson and Liang (1995) noted that the implications of the growth entrapment model extend well beyond sector zoning, and that the entrapment process could operate in any situation where the composition of the mineral surface differs from that of the bulk lattice. Watson (1996) later discussed the broader implications of the model, emphasizing that, because the occurrence of growth entrapment depends on the outcome of the competition between growth rate (V) and lattice diffusivity (D), the process may dominate trace-element uptake into minerals that grow rapidly under conditions where near-surface diffusion is slow. In this respect, calcite growing in seawater is a prime candidate for growth entrapment— especially given that this mineral is known to exhibit selective surface enrichment with respect to some ions (e.g., Paquette and Reeder, 1995; Reeder, 1996). Because the growth entrapment model does not involve diffusive boundary-layer effects in the growth medium, it can operate under circumstances where diffusion in the growth medium is fast, as is the case for ions in seawater.

In closing this section, it should be noted that over the past few decades there has been considerable interest among materials scientists in the uptake of impurities in growing crystals (see, e.g., Aziz, 1982; Tiller, 1991). Tiller and Ahn (1980) tackled essentially the same problem that was addressed by Watson and Liang (1995), but the exact steady-state solutions they obtained do not address impurity concentration in the crystal interior, which is the main information of geochemical interest. More recent models (e.g., Aziz, 1996; Ahmad et al., 1998) address "solute trapping" at very high growth rates.

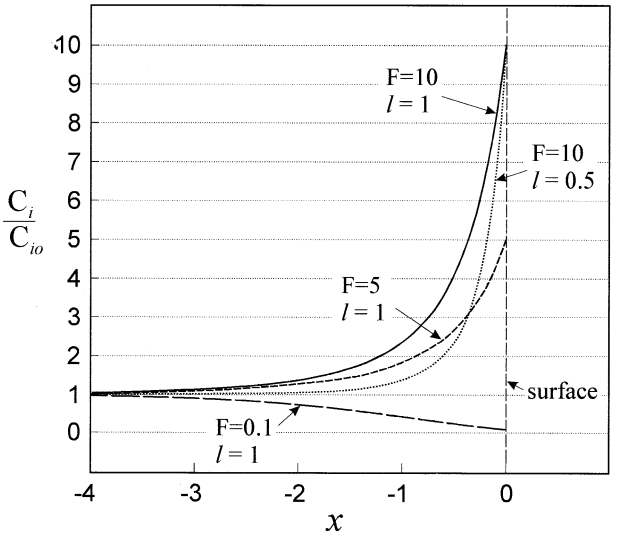

Fig. 1. Form of the equilibrium near-surface enrichment and depletion profiles (Eqn. 1) assumed in the modeling. See text for symbols and discussion.

2.2. Details, General Implications, and Limitations of the Model

As the starting point for their mathematical analysis, Watson and Liang (1995) regarded surface enrichment under static conditions (i.e., V = 0) as an equilibrium phenomenon that can be described in terms of a spatially variable chemical potential or activity coefficient in the crystal. Following Tiller and Ahn (1980) they assumed that the activity coefficient decreases exponentially near the crystal surface, resulting in an exponentially increasing concentration approaching the surface:

$$C_i = C_{io}F^{\exp(x/l)} \quad (1)$$

where C_i is the concentration of element$_i$ at some distance x from the surface, C_{io} is the concentration reflecting partitioning equilibrium with respect to i between the crystal lattice and the growth medium at infinite distance from the surface, l is the half-thickness of the enriched surface layer, and F is the surface enrichment factor (effectively a partition coefficient for the crystal surface relative to the crystal interior). Note that in the formulation represented by Eqn. 1, x is zero at the surface and increases to negative numbers moving into the crystal. Figure 1 illustrates C_i vs. x curves given by Eqn. 1 for a few values of F and l. It is emphasized that as long as the crystal is neither growing nor dissolving, these concentration profiles represent equilibrium. Element i is enriched in the near-surface because this region is structurally distinct from the bulk lattice and more accommodating to some impurities (see discussion in section 3.2 re. calcite specifically).

A few additional points should be made with reference to Figure 1, as these will become significant later in the paper. The first is that the exact form of the equilibrium C_i vs. x curve is not important to the overall behavior of the system when the crystal begins to grow: its width (l) and height (F) are important, but functional forms other than the exponential represented by Eqn. 1 yield similar entrapment behavior during growth (Watson and Liang, 1995). It is also important to

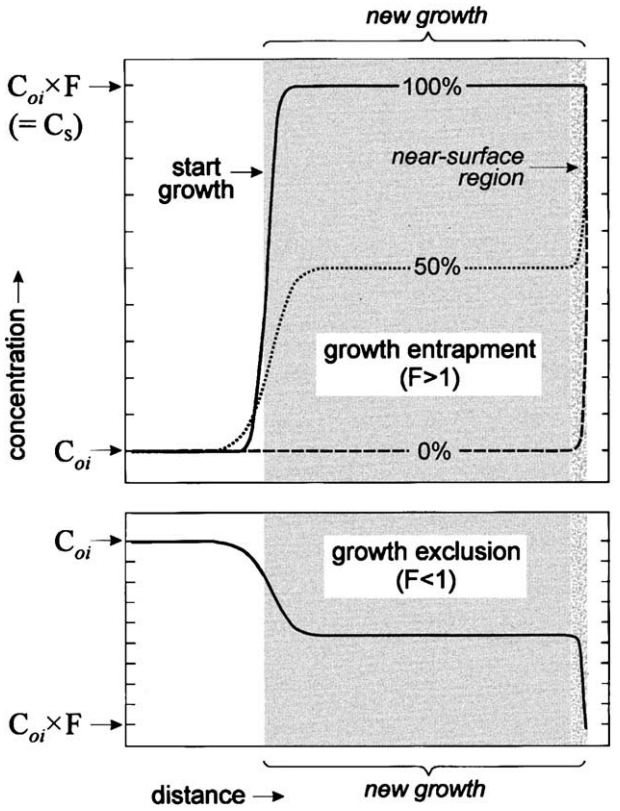

Fig. 2. Concentration profiles representing three growth-entrapment efficiencies (top panel). If entrapment is 100% efficient, the newly grown crystal preserves the composition of the surface within the bulk lattice. Bottom panel illustrates "growth exclusion," which occurs when the surface enrichment factor, F, is less than 1.

emphasize that there is no reason why F must be restricted to values greater than 1—i.e., equilibrium *depletion* in the near-surface region is equally plausible as near-surface enrichment, so F<1 is possible. The near-surface region has characteristic structural, chemical and transport properties (see section 3.2), so the possibility that some elements will be less compatible in the near-surface than in the bulk lattice is not unreasonable. Lastly, it is a key assumption in the growth entrapment model that equilibrium C_i vs. x curves like those in Figure 1 exist solely because of proximity to a "free" surface (or an interface against fluid); accordingly, as the crystal grows, the equilibrium profile will attempt to move with the advancing interface. In order for the profile to migrate unchanged in form and "attached" to the interface, however, diffusion of *i* in the near-surface region must be fast enough to continuously redistribute *i* at the length-scale of *l*. To the extent that diffusion is unsuccessful in doing this, growth entrapment occurs (i.e., the chemical characteristics of the near-surface region are preserved to some extent in the bulk lattice). Note that if the near-surface region is *depleted* in *i* relative to the equilibrium partitioning value C_{oi} (i.e., if $F < 1$), then inefficient diffusion would lead to "growth exclusion" of *i*.

The reader is referred to Watson and Liang (1995) for the mathematical details of the growth entrapment model. Briefly summarized, the approach was to define the chemical potential of *i* as a function of distance, and on the basis of this relationship write a non–steady state diffusion/mass conservation equation (their eqn. 9) constrained by appropriate initial and boundary conditions. Watson and Liang then solved the nondimensionalized equation numerically on a fixed grid using an explicit finite-difference method. The results are most easily described and generalized in terms of a nondimensional "growth Péclet number" for the surface layer:

$$\mathrm{Pe} = \mathrm{V} \cdot l/\mathrm{D} \qquad (2)$$

where V is the growth rate, l is the half-thickness of the near-surface layer enriched in *i*, and D is the diffusivity of *i*. This nondimensional number represents the ratio of the diffusive time scale (l^2/D) to the growth time scale (l/V) and its value largely determines the effectiveness of growth entrapment (that is, the extent to which a crystal takes on the chemical characteristics of its surface). (Note that Watson and Liang, 1995, conceived of D in the conventional sense—i.e., as characterizing site-to-site hopping of ions through the crystal lattice—but it can be used in a more general way to describe ion mobility by any mechanism; see section 3.2.1.) Figure 2 is a schematic diagram illustrating three growth entrapment efficiencies (0%, 50 and 100%) and one example of growth exclusion. Figure 3 summarizes entrapment behavior for a range of Pe and three values of F. The main conclusions from the figure are that some growth entrapment can occur at Pe values as low as 0.1, and that substantial entrapment is inevitable at Pe ≥ 10. Entrapment efficiency is weakly dependent on F in the sense that the "threshold" value of Pe required for some growth entrapment is lower for smaller F.

For more extensive discussion of the general geochemical and petrologic implications of Figure 3, the reader is referred to Watson (1996). The author emphasized that even if the principles embodied in the growth entrapment model are "correct," there are obstacles to its quantitative use in un

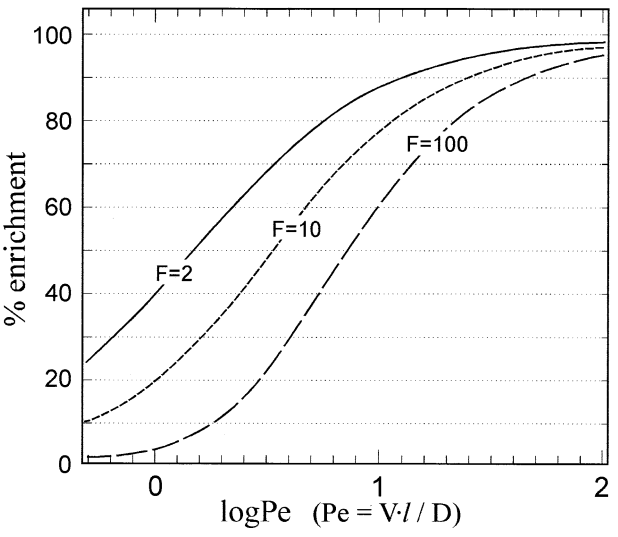

Fig. 3. Lattice enrichment in a growing crystal as a function of the dimensionless growth Péclet number Pe (= V · l/D). The enrichment level at a given value of Pe is represented by a concentration plateau like those shown in Figure 2. Following Watson and Liang (1995), % enrichment is calculated as $(C_i/C_{oi}-1)/(F-1)\times 100$. See text for discussion.

derstanding trace element uptake during crystal growth, simply because the values of key parameters are largely unknown. This is particularly true of F, D and *l*; V can often be constrained within reasonable bounds in laboratory growth experiments, or by time-integration of observed sizes of natural crystals (the presence or absence of growth entrapment is relatively insensitive to the value of F, although the *extent* of enrichment does depend on F; see Fig. 3). The data base for ion diffusivities in mineral lattices (including calcite) is growing rapidly, but it is also becoming increasingly clear that ions can be much more mobile in the near-surface region than in the bulk lattice at some distance from the surface (e.g., Stipp et al., 1992; Hoffmann and Stipp, 2001; see section 3.2.1).

In this paper, existing experimental data on trace-element uptake during calcite growth are used to evaluate the overall consistency of the growth entrapment model with laboratory measurements.

3. A TEST OF THE MODEL USING LABORATORY DATA ON TRACE-ELEMENT UPTAKE

3.1. General Strategy

To remain viable, a model must be consistent with observed behavior of a real system. The experimental data of Lorens (1981) and Tesoriero and Pankow (1996) on trace-element uptake in calcite provide a means not only to assess the performance of the growth entrapment model but also to evaluate the appropriateness of additional assumptions about transport and partitioning processes in the near-surface region of a crystal during growth. The strategy pursued below is to treat the body of laboratory growth/partitioning data as both a guide to the modeling approach and a simulation objective.

Following Watson and Liang (1995), the entrapment of trace elements during growth is modeled by solving the appropriate diffusion equation (cf. no. 9 of Watson and Liang) using the explicit finite-difference method (e.g., Crank, 1975). The numerical algorithm used here is slightly different from that of Watson and Liang in that, rather than simulating growth by moving the interface through a fixed grid, the diffusion profile is translated through the grid in the direction opposite the growth direction. In this moving reference frame, the diffusion equation solved numerically is

$$\frac{\partial C_i}{\partial t} = \frac{\partial}{\partial x}\left[D\frac{\partial C_i}{\partial x}\right] - \frac{\ln F}{l}\left[C_i D \exp\left(\frac{x}{l}\right)\right] + V\frac{\partial C_i}{\partial x} \quad (3)$$

Before running simulations for this study, it was confirmed that the present approach and that of Watson and Liang (1995) give indistinguishable results. However, the comparison did uncover a point of possible confusion over semantics that was not addressed in the initial paper: here, "*l*" is the dimensional parameter actually used to specify the width of the chemically anomalous near-surface region in the simulations. As shown in Figure 1, the size of *l* is only about half the total width of the region, hence the use of the term "half-thickness" in the earlier papers.

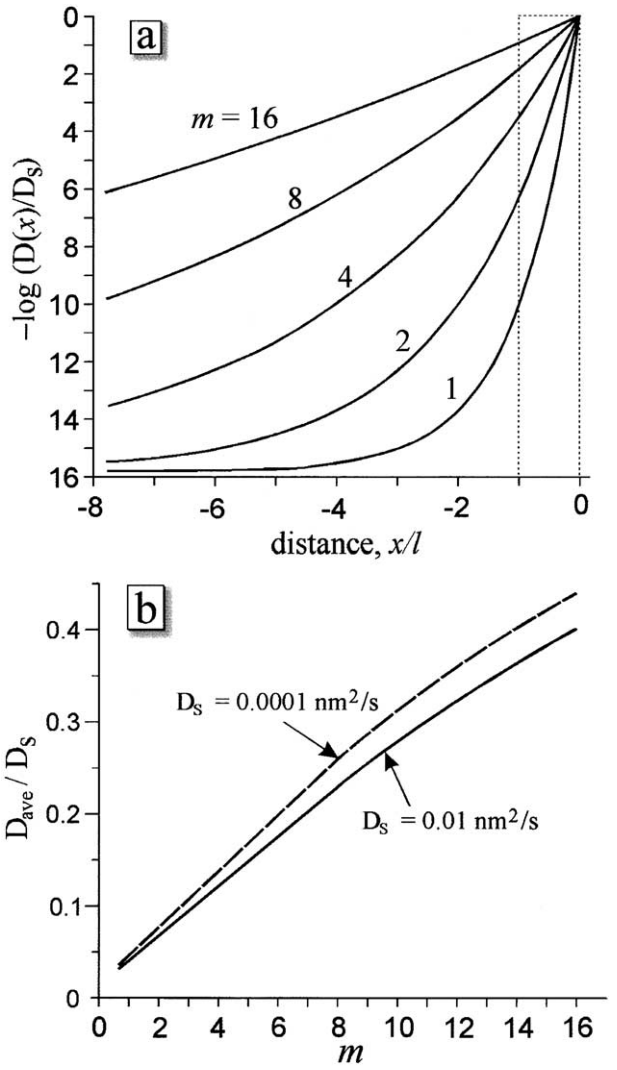

Fig. 4. (a) Variation in diffusivity with depth according to Eqn. 4 for several values of *m*. Diffusivities are normalized to a surface value, D_S, of 10^{-2} nm^2/s. The normal lattice diffusivity, D_l—obtained by down-temperature extrapolation of experimental data (Cherniak, 1997)—is set at 1.53×10^{-18} nm^2/s. Variation in D(*x*) over the region critical to the model ($-1 < x/l < 0$; see dotted box) is relatively insensitive to the choice of D_S. This is shown in (b), where the diffusivity averaged over distance *l* (i.e., D_{ave}) is plotted against *m* for two values of D_S.

3.2. New Assumptions and Constraints

3.2.1. Diffusion

Stoll et al. (2002) conducted what amounted to a test of consistency between the Watson/Liang growth entrapment model and the growth rate versus (apparent) partition coefficient data of Lorens (1981) and Tesoriero and Pankow (1996), specifically for Sr. They concluded that the experimental data conform in a general way to the predictions of the model (see their fig. 4), but they also realized that conformance can be achieved only if the diffusivity of Sr in the near-surface region of calcite is much higher than measured values for D_{Sr} in the calcite lattice (Cherniak, 1997). If the growth entrapment model is an accurate representation of diffusion/partitioning dynamics in the near-surface region

during growth, then D_{Sr} in this region must fall between $\sim 10^{-3}$ and 10^{-1} nm^2/s, assuming $l \sim 1$ nm. This is roughly 16 orders of magnitude higher than Cherniak's (1997) value of D_{Sr} for the calcite lattice extrapolated down to the 25°C temperature of the experiments. This is a huge discrepancy, but it does not necessarily call into question any of the relevant experimental data *or* the growth entrapment model. The optimistic (preferred) interpretation is simply that Sr is much more mobile in the structurally distinct near-surface region than in the "normal" lattice. This interpretation is not only reasonable but also reassuring: given the surface-site selectivity shown by Sr (Paquette and Reeder, 1995), and assuming the growth entrapment model has any validity at all, then "normal" lattice diffusivities would preclude attainment of calcite/seawater equilibrium under all circumstances.

The question, then, is whether there is any evidence for rapid diffusion or high mobility of ions in the near-surface region of calcite. At this point, the evidence appears to be mixed. Stipp et al. (1992) examined near-surface mobility of Cd^{2+} by monitoring changes with time in the near-surface concentration of Cd introduced onto a cleaved calcite surface. The changes were dramatic in the time frame of hours to days, implying rapid migration into the solid. Modeled as a thin source diffusing into the calcite, the observed diminution rate of Cd concentration implies a minimum diffusivity on the order of 10^{-4} nm^2/s, averaged over the information depth of ~30 Å (see data in table 6 of Stipp et al., 1992). As Stipp and coworkers showed in subsequent papers (Stipp, 1998; Stipp et al., 1998; Hoffmann and Stipp, 2001), not all ions are as mobile in the surface region as Cd appears to be. However, several other ions—Zn^{2+}, Ni^{2+}, Na^+, K^+, and Cl^-—were shown by these workers to be mobile in the near-surface region of calcite at room temperature. The actual migration mechanisms and pathways vary, as several fundamentally different phenomena appear capable of redistributing ions. Mechanisms include migration along defects extending relatively deep into the crystal (Stipp et al., 1998) and local dissolution/reprecipitation (recrystallization) that rearranges atoms in the surface itself, leading to burial of ions initially at the immediate surface (Hoffmann and Stipp, 2001). The extended defect mechanism may not be relevant to the present problem, and in any case is likely to vary from one crystal to another. The spontaneous recrystallization mechanism, although not solid-state diffusion in a mechanistic sense, is nevertheless able to redistribute ions in the direction perpendicular to the general plane of the surface (i.e., the x-direction in the present model). Ion redistribution by any and all of these mechanisms can be described in terms of a diffusivity—i.e., a constant of proportionality between a flux and a chemical potential gradient that is nonspecific as to the mechanism of atom migration.

A different perspective on ion mobility in the near-surface of calcite at room temperature is provided indirectly by the work of Cheng and coworkers (see summary in Bedzyk and Cheng, 2002), who used X-ray standing waves to investigate cation sorption on calcite surfaces (Co^{2+}, Ni^{2+}, Cu^{2+}, Zn^{2+}, Cd^{2+}, Pb^{2+}, $UO_2{}^{2+}$). With measurement times of up to a week per sample, no diminution of the impurity ion signal over time was noted in these studies, implying significantly more sluggish near-surface transport than deduced for some ions by Stipp and coworkers (though no actual estimates of diffusion rates could be obtained from the X-ray standing wave studies). In summary, the body of evidence available at present suggests that some ions are mobile in the near-surface region of calcite under some circumstances. Stipp and coworkers have extended to other elements the earlier conclusion of Davis et al. (1987), based on the rate of ^{45}Ca uptake into calcite at 25°C, that Ca^{2+} can be much more mobile in the near-surface region than in the calcite lattice. As the studies of Stipp and coworkers and Fenter et al. (2000) have clearly shown, this higher near-surface mobility should not be interpreted to mean that there exists an amorphous, possibly hydrated layer at the calcite surface. The transition from aqueous growth medium to calcite lattice is definite and abrupt, but the near-surface should be understood as a dynamic region in which at least some ions redistribute themselves effectively even at ambient temperature. In the context of the present conceptual model, an intuitively useful—if not entirely accurate—image of the near-surface region of a growing calcite crystal is a "gardening zone" of constant thickness that advances into the aqueous medium as the crystal grows. This moving, dynamic zone is where the immediate surface composition of the crystal is converted into that acquired by the lattice behind it.

The measured growth-rate dependence of trace-element uptake in calcite (Lorens, 1981; Dromgoole and Walter, 1990; Tesoriero and Pankow, 1996) and the documentation of high near-surface ion mobility by Stipp and coworkers (Stipp et al., 1992, 1998; Hoffmann and Stipp, 2001) warrant a refinement of the growth entrapment model of Watson and Liang (1995) as it might apply to calcite. The original model assumed uniform mobility of ions regardless of proximity to the surface. Down-temperature extrapolation of lattice diffusion data for calcite (e.g., Kronenberg et al., 1984; Farver, 1994; Farver and Yund, 1996; Cherniak, 1997; Fisler and Cygan, 1999; Labotka et al., 2000; Kent et al., 2001) implies virtual immobility of ions in the lattice at ambient conditions, a conclusion supported by the preservation of fine chemical zoning features over geologic time scales. It now seems likely, however, that at least some ions are relatively mobile in the near-surface at ambient temperatures, which leads to the conclusion that the mobilities of trace elements in calcite vary with proximity to the surface over some distance interval. In retrospect this seems reasonable, but it is not obvious how exactly to address the complication in the modeling. The approach taken below is to express ion mobility, regardless of specific mechanism, in terms of a diffusivity that varies with distance from the surface, in the same manner as was done for the chemical potential (Watson and Liang, 1995) and equilibrium concentration (Eqn. 1). Accordingly, the diffusivity is assumed to conform to

$$D(x) = D_l\{(D_s/D_l)^{\exp[x/(m \cdot l)]}\} \quad (4)$$

where D is the diffusivity at some distance x from the surface, D_l is the diffusivity in the "normal" lattice (i.e., far removed from the surface), and D_S is the diffusivity at the immediate surface. The parameter l has the same significance as in Eqn. 1 (i.e., the thickness of the enriched or depleted layer; Fig. 1) and m is simply a multiplier relating the width of the chemically distinct layer to that of the high-diffusivity region ($m = 2$ means the high-diffusivity region is twice the thickness of the chemically distinct layer). There is little basis upon which choose a value for m, so several choices are used in the models below in order assess differences in overall behavior.

The value for the normal lattice diffusivity D_l was calculated by down-temperature extrapolation of published lattice diffusion values for Sr (1.53×10^{-18} nm^2/s; see Cherniak, 1997), but the specific choice of an Arrhenius relation is almost immaterial because the room temperature values are so low in all cases. The surface diffusivity D_S was assumed to be 10^{-2} nm^2/s for most of the simulations described below, but it was also confirmed that behavior of the system is the same for any assumed value of $V \cdot l/D_S$. The use of a very high diffusivity at x∼0 is not crucial to the success of the model; it is the combination of all three parameters (V, *l*, and D_S) that determines outcome. Moreover, D_S applies only at the literal surface of the crystal; the diffusivity governing atom mobility in the near-surface should be understood as a laterally averaged quantity that drops precipitously even over a distance of one monolayer (see Eqn. 4 and section 3.2.3). Figure 4a shows D(*x*) as a function of normalized depth (*x*/*l*) for several values of *m* when $D_S = 0.01$ nm^2/s. These curves would vary somewhat with choice of D_S (see Eqn. 4) but, as discussed in section 3.4, the critical distance interval is *l*, and $D(x)/D_S$ is relatively insensitive to choice of D_S over this interval. This point is illustrated in Figure 4b, which shows the average diffusivity in the region defined by *l* as a function of *m* for two different choices of D_S. This figure emphasizes, also, that the average diffusivity in the near surface region is significantly lower than D_S.

3.2.2. *Thickness of the Enriched (or Depleted) Layer*

Since publication of the growth entrapment model, new analytical techniques and computer simulations have shed light on the atomic structure of the near-surface regions of minerals, calcite among them. Fenter et al. (2000) concluded from in situ X-ray reflectivity studies of the calcite/H_2O interface that deviations from the "normal" lattice structure extend only ∼2 monolayers (0.6 nm) into the crystal. In other words, it is only in the outermost 2 monolayers that atom positions are slightly but measurably "relaxed" from their usual coordinates in the calcite unit cell (see also Rohl et al., 2003). The distorted nature of the lattice sites may mean that this 0.6-nm region is also distinct in terms of trace-element composition and diffusion characteristics. In this respect, the information provided by the X-ray reflectivity results may set a lower bound to the thickness of the anomalous near-surface region. Setting a realistic upper bound to the value of *l* is more difficult. Calcite growth by the spiral mechanism produces asymmetric growth hillocks, which create both general "topography" on the advancing interface and specific types of step sites on the surface (Paquette and Reeder, 1995; Reeder, 1996; Teng et al., 2000; Reeder et al., 2002). During growth, the concentration of a specific element on the surface itself is determined by the nature and density of specific step sites (Reeder, 1996). The 0.6-nm "relaxed" region beneath may allow a surface concentration anomaly to extend a few monolayers into the crystal. It must also be recognized that this anomaly follows the topography of the hillocky surface, so *l* could be viewed as "stretched" in the x-direction when the entire growth surface is taken as the plane of interest for modeling purposes.

For most of the numerical simulations run in the present study, a surface layer thickness (*l*) of 0.5 nm was used in conjunction with a surface diffusivity (D_S) of 10^{-2} nm^2/s (see section 3.2.1). This choice was made because the resulting value of l/D_S (= 50) leads to variation in cation partition coefficients with growth rate over the range in V where similar changes are observed by experiment. Once again, however, because it is the dimensionless parameter $V \cdot l/D_S$ that determines behavior, the results can be readily adjusted to any desired value of *l* and/or D_S.

3.2.3. *Lateral Averaging of Chemical and Transport Properties*

Given the values of *l* and *m* considered plausible in this study, some readers may recognize that element concentrations and diffusivities are assumed to vary markedly across a single monolayer of the calcite structure. In other words, the calcite lattice is represented as a continuum even at a length scale much smaller than the ions comprising that lattice. Clearly, properties such as C_i and D cannot actually change across a single atom or molecule. However, it is appropriate to consider them as doing so in a case where a 1-dimensional modeling approach is used to simulate behavior of a system that exhibits variability perpendicular to the direction of primary interest. Variability in the plane of the advancing calcite/H_2O interface takes the form of gentle topography—i.e., stepped spiral hillocks around screw dislocations and other imperfections (see, e.g., Teng et al., 2000). This topography leads, in turn, to lateral chemical variability and differences in D that reflect the immediate environment of a specific ion. The present model treats C_i and D as functions solely of *x*, implicitly assuming that the values of C_i and D at a given *x* coordinate represent averages over the y-z plane at that particular value of *x* (see Fig. 5). No actual averaging procedure is used in the present simplistic treatment, but refinements may be possible when more detailed information becomes available on impurity incorporation and diffusion in the near-surface region of calcite (see discussion of averaging in chapters 9 and 10 of Drew and Passman, 1998).

Although introduced specifically to illustrate averaging, Figure 5 also calls attention to a related complexity of the overall growth entrapment problem that has been ignored up to this point: i.e., that the surface enrichment factor, F, may depend upon V. As noted previously, impurities bond preferentially at step sites (e.g., Paquette and Reeder, 1995), so the equilibrium impurity concentration may depend upon the density of steps on the surface of interest. Because the nature of the steps (e.g., the terrace width), and therefore the density of step sites, can depend upon V (as well as other factors—see Teng et al., 2000), F is also likely to depend on V. Because faster growth leads to narrower terraces (thus providing more step sites?), F may be a positive function of V. The possibility is noted in the interest of completeness, but no assessment is made of the consequences to "enrichment vs. Pe" curves like those shown in Figure 3, simply because any choice of $F = f(V)$ would be totally arbitrary. However, it seems entirely possible that a curve representing a specific system could have a steeper or shallower slope than the curves shown in Figure 3 due to a growth-rate dependent F.

3.3. Calcite/H_2O Partitioning of Cations at Variable Growth Rates

Stoll et al. (2002) summarized experimentally determined data for the apparent partition coefficient of Sr (K_{app}(Sr))

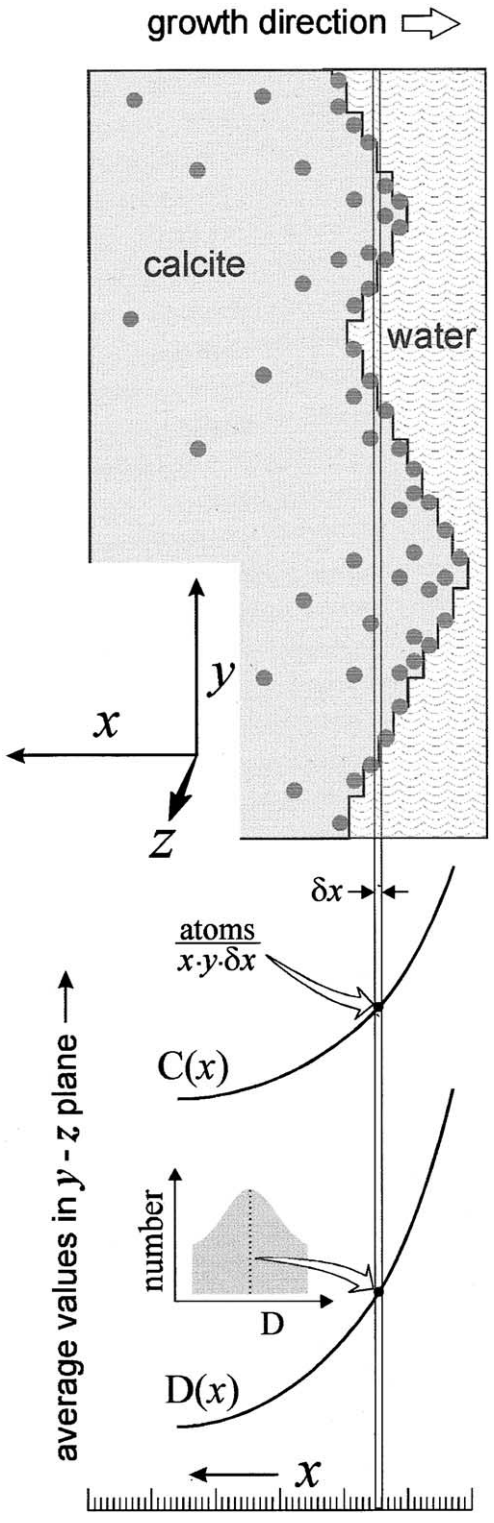

Fig. 5. Schematic illustration of the calcite/H_2O interface during growth, with coordinate system in the inset. Growth progresses in the x-direction, but there is lateral variation of calcite properties in the *y*-*z* plane due to surface topography (greatly exaggerated). The thin vertical window perpendicular to the growth direction represents a section through a *y*-*z* "plane" of finite thickness δx. Local concentration and diffusivity (C_i and D) must vary with $_y$ and *z*, so their values at any given *x* in the numerical model represent averages, as suggested at the bottom of the figure. This lateral averaging means that C_i and D in the model can change smoothly (and steeply) across a single monolayer of the calcite structure. See text for discussion and implications.

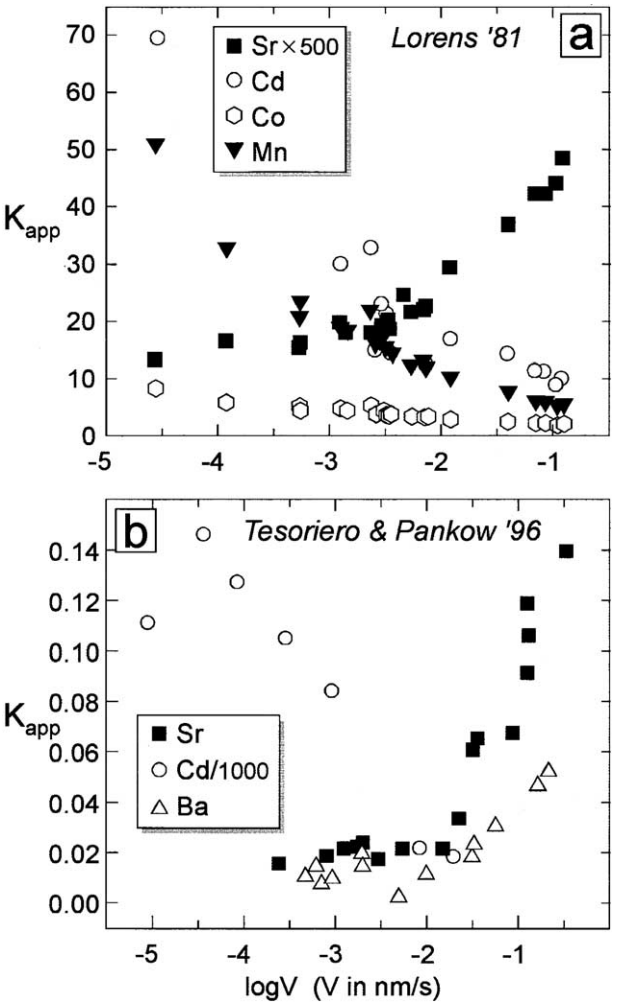

Fig. 6. Apparent partition coefficients (K_{app}) *vs.* growth rate for five elements: laboratory data of (a) Lorens (1981) and (b) Tesoriero and Pankow (1996).

versus growth rate published earlier by Lorens (1981) and Tesoriero and Pankow (1996). The original studies also yielded data for Ba, Cd, Co and Mn, which are shown in Figure 6 along with the Sr data. It must be emphasized that the data reported in the original experimental studies are partition coefficients and *molar precipitation rates* (nmol/min-mg). In Stoll et al. (2002) and in the present treatment, these precipitation rates were converted into linear growth rates (V) to generate K_{app} vs. logV plots. This conversion necessitates assumptions whose validity cannot be tested without specific knowledge of crystal size distributions and nucleation processes in the experiments, so Figure 6 must be regarded as a qualitative representation of partitioning vs. growth rate behavior. This limitation aside, Stoll et al. (2002) noted that the Sr data are qualitatively consistent with the model curves in Figure 3, assuming Sr is enriched in the surface layer relative to the concentration in calcite dictated by the equilibrium partition coefficient, K_d(Sr) [the near-surface enrichment factor, F, is not known, but Paquette and Reeder, 1995, have shown that Sr concentrations vary spatially on a calcite growth faces due to local availability of surface sites]. Both the Lorens (1981) and Tesoriero and Pankow (1996) data show a lack of dependence of K_{app}(Sr)

upon V at growth rates of 0.01 nm/s or lower. As concluded by the authors, this behavior suggests that the equilibrium K_d is achieved at low precipitation rates. If the growth entrapment model is a reasonable representation of the dynamics of the system, this can be interpreted to mean that Sr diffusion is fast enough in the near-surface to maintain the equilibrium concentration profile (Fig. 1) during growth at 0.01 nm/s or slower (i.e., no growth entrapment occurs).

Barium exhibits behavior similar to that of Sr in the sense that growth rates above 0.01 nm/s appear to result in some entrapment, leading to high K_{app}(Ba) values. All other elements (Cd, Co, Mn) show behavior that is markedly different from that of Sr and Ba in two respects: 1) K_{app} values decrease (rather than increase) with increasing growth rate, and 2) equilibrium K_d values are never achieved, because K_{app} depends on V over the entire range of rates examined (~6 orders of magnitude).

The first of the two differences noted above can be explained in a simple way by the growth entrapment model: the negative slopes of the K_{app} versus V plots for Cd, Co and Mn are the result of *depletion* of these elements in the near-surface region rather than enrichment (i.e., F is less than 1). In other words, the experimental data are revealing the consequences of "growth exclusion" as opposed to growth entrapment. This interpretation seems reasonable given the sizes and qualitatively known partitioning behavior of the five ions represented in the overall experimental data set. As relatively large ions substituting for the smaller Ca^{2+}, Sr^{2+} and Ba^{2+} are relatively incompatible in the calcite lattice and better accommodated in the more flexible environment of the near-surface region. In contrast, Cd^{2+}, Co^{2+} and Mn^{2+} are similar in radius or smaller than Ca^{2+} and extremely compatible in the calcite lattice. These ions presumably are stabilized in the normal calcite lattice relative to the near-surface region, much in the way that highly compatible substituents in magmatic silicate minerals prefer the crystal lattice to the contacting melt. The model simulations described below will show the consequences of F<1.

The second difference in behavior of the two groups of elements—i.e., the apparent failure of Cd, Co and Mn to reach partitioning equilibrium at even the slowest growth rates—seemed initially to pose a problem for the growth entrapment model. The potential problem hinges on the presumed relative diffusivities of the ions under consideration: considered in the context of a vast amount of information on ionic diffusion in condensed phases, the diffusivities of Cd, Co and Mn might be inferred to be higher than those of Sr and Ba. In a given diffusion matrix (crystal, melt, or glass), diffusion of small ions is faster than diffusion of larger ions of the same charge. As shown in Figure 7, this generalization is more or less borne out by comparison of existing data for cation diffusion in the calcite lattice (e.g., Mg^{2+} diffuses faster than Sr^{2+} and Pb^{2+}). Actual data on relative diffusivities in the near-surface region of calcite are lacking, so it is by no means definite that small ions are more mobile than larger ones in the region of interest here. Assuming for the moment that cation diffusivity *is* inversely proportional to cation size, then the apparent failure of smaller ions (Cd^{2+}, Co^{2+} and Mn^{2+}) to reach partitioning equilibrium at low growth rates needs explaining. There are two possibilities: 1) the depth-dependence of D varies from one ion to another (this is not implausible, but no data are available); and 2) in terms of the range of growth rates over which

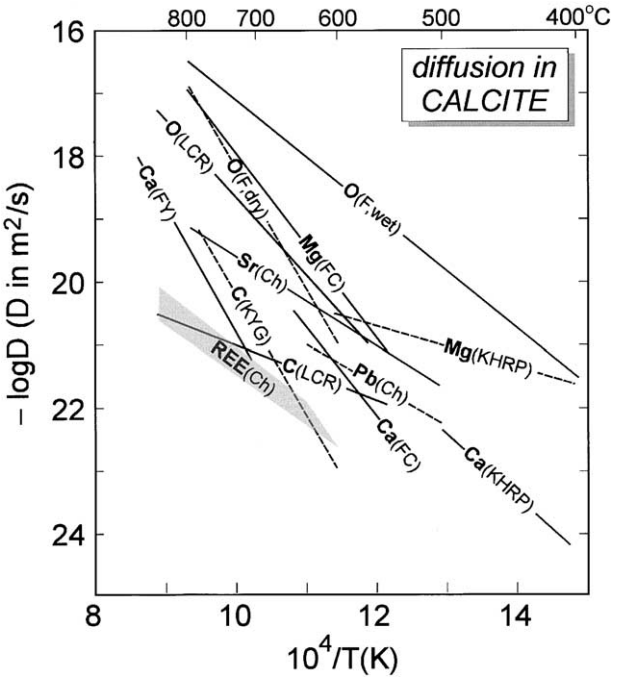

Fig. 7. Summary of lattice diffusion data for calcite. Chemical symbols are bold, abbreviations of data sources are as follows: Ch = Cherniak (1997); F = Farver (1994); FC = Fisler and Cygan (1999); FY = Farver and Yund (1996); KHRP = Kent et al. (2001); KYG = Kronenberg et al. (1984); LCR = Labotka et al. (2000).

K_{app} depends upon V, the behavior of the model is different for $F < 1$ relative to $F > 1$. The next section will show that the latter possibility is true, although this does not preclude the former being true as well.

3.4. Illustrative Models with D = *f*(*x*)

Numerical simulations of trace-element uptake during calcite growth were run at growth rates similar to those of the laboratory studies, seeking consistency of the model with the experimental results. In addition to the assumptions noted in section 3.2, it was further assumed that F = 10 (surface enrichment) or 0.1 (surface depletion). These choices of moderate near-surface enrichment or depletion are made because they are consistent in magnitude with observed sectoral concentration differences in calcite (e.g., Reeder, 1996; Paquette and Reeder, 1995). The impact of using other values can be assessed by reference to Figure 3 or by making adjustments with the knowledge that the results are the same for a given value of $Pe = V \cdot l/D_S$.

Figure 8 is a summary of growth entrapment curves for F = 10 and *m* values ranging from 1 to ∞ (*m* = ∞ corresponds to the case examined by Watson and Liang, 1995, and discussed by Watson, 1996). The vertical axis of the figure, labeled $\mathbf{K}_A$, is the apparent partition coefficient (K_{app}) divided by the equilibrium partition coefficient (K_d). It is clear from this figure that the behavior of the system is sensitive to the choice of *m*. If the width of the high-diffusivity region is coincident with that of the chemically anomalous region (*m* = 1), then the apparent partition coefficient varies continuously over the entire range of growth rates considered, and the equilibrium K_d is never ap-

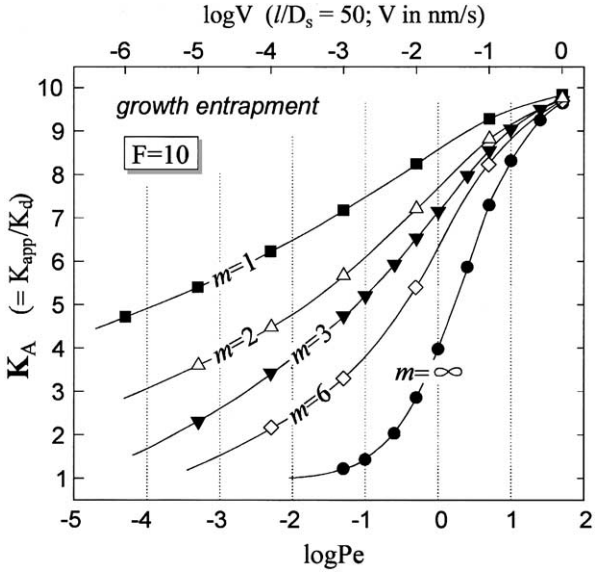

Fig. 8. Growth entrapment curves for F = 10 showing the effect of varying *m* (*m* is the width of the high-diffusivity region ratioed to that of the chemically anomalous region). The case of $m = \infty$ corresponds to previous models of Watson and Liang (1995). $\mathbf{K}_A$ is the ratio of the apparent partition coefficient, K_{app}, to the equilibrium partition coefficient, K_d. Pe is the "growth Péclet number," given by $V \cdot l/D_S$. In this and similar figures (nos. 9 and 13), the upper x-axis scale is in units of logV for the specific case of $l/D_S = 50$; this choice puts V in the range covered by experimental studies (Fig. 6). See text for discussion.

proached—even at the slowest growth rate (lowest Pe) considered. This contrasts with the case of m = ∞, where $\mathbf{K}_A$ changes from ~1 to ~10 over just three orders of magnitude increase in V.

Figure 9 shows the results of simulations analogous to those represented in Figure 8 but with F = 0.1—i.e., the surface depletion case, as might pertain to the behavior Cd, Co and Mn. Despite general "symmetry" with the curves in Figure 8, some major differences are evident. For $m = \infty$, the sigmoid $\mathbf{K}_A$ vs. logPe curve shows relative changes comparable with those for the analogous curve in Figure 8. However, the curves for low values of *m* are much flatter, indicating significantly less sensitivity of $\mathbf{K}_A$ to growth rate, and complete failure to approach the equilibrium K_d at all growth rates considered. A potentially significant conclusion from this comparison is that, in cases where D varies with proximity to the crystal surface (which, it is claimed here, it must do), *partitioning equilibrium may be achieved more easily for surface-enriched elements (e.g., Sr and Ba) than for surface-depleted elements (e.g., Cd, Co and Mn)*. The behavior differs for the two cases because of the marked difference in the nature of near-surface concentration profiles and the superposition upon them of a spatially varying diffusivity. The potential significance of the result is that, for some growth conditions, species that may diffuse more slowly (e.g., Sr^{2+} and Ba^{2+}) can achieve their equilibrium K_d values under circumstances when faster-moving ions do not. The inset in Figure 9 shows the experimental data of Lorens (1981) for Mn in comparison with a model K_{app} vs. logPe curve generated using F = 0.1 and an equilibrium partition coefficient (K_d) of 55. Reasonable agreement is achieved when *m* is arbitrarily set at 9. However, this should not be regarded as a unique "fit" to the data, mainly because K_d is not actually known.

A remaining question concerning growth entrapment with spatially variable D is the sensitivity of the overall behavior to the choice of a specific functional dependence of D upon *x*. Eqn. 4 was used for most simulations because of its mathematical similarity to the assumed form of the equilibrium compositional anomaly (Eqn. 1). Simpler expressions for $D = f(x)$ were also explored, including

$$D(x) = D_l + (D_s - D_l)\exp\left[\frac{x}{m \cdot l}\right] \quad (5)$$

This expression leads to variation of $\mathbf{K}_A$ with growth rate in a manner very similar to that summarized in Figures 8 and 9. However, the values of *m* required to produce the same behavior are markedly different. The "$m = 1$" and "$m = 6$" curves in Figure 8, for example, are well approximated with $m \sim 0.03$ and $m \sim 0.17$, respectively, when $D(x)$ is described by Eqn. 5. Given the similarity in overall behavior—and lacking actual knowledge of the manner in which D varies with *x* (or even whether the dependence is the same for all ions)—there is no strong reason to prefer either equation as a description of $D(x)$. Eqn. 5 is simpler, but Eqn. 4 is more consistent with the form of the equilibrium compositional anomaly in the near-surface originally assumed by Watson and Liang (1995). The one aspect of the dependence of D upon *x* that is crucial to the "stretching" of the $\mathbf{K}_A$ vs. logPe curves is significant variation in D across the near-surface region as defined roughly by *l*. This point is emphasized in Figure 10, in which $\mathbf{K}_A$ is plotted against logPe for the case where $m = 2$ and $D(x)$ is constant over *l* but drops exponentially moving deeper into the crystal. In this case, $\mathbf{K}_A$ deviates from the $m = \infty$ case only at logPe < 0.

The general conclusion to be drawn from the new simulations of trace-element uptake is that the growth entrapment model can explain all the salient aspects of the existing data, given the existing latitude in choice of modeling parameters. Alternative growth-rate based, abiogenic explanations cannot do this. In principle, trace-element uptake can depend on growth rate when the crystal interface advances fast enough to perturb the concentration in the immediately contacting growth

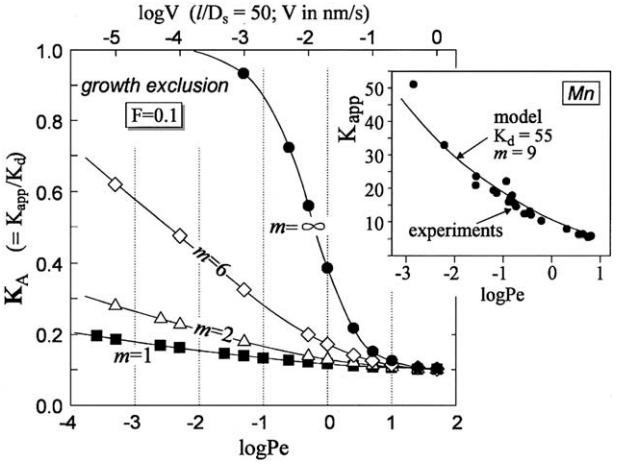

Fig. 9. "Growth exclusion" curves resulting from F = 0.1. Symbols and other parameters are as in Figure 8. The inset shows that with the right (but nonunique) choice of parameters (K_d = 55; F = 0.1; *m* = 9), the model can produce results very similar to actual experimental measurements—the Mn data of Lorens (1981).

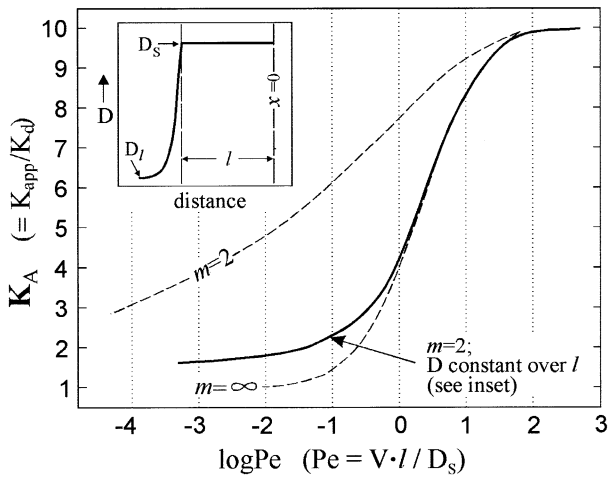

Fig. 10. K_A vs. logPe for the case where $m = 2$ and D(x) is constant over l as in the inset (solid curve). This is compared to similar $\mathbf{K}_A$ *vs.* logPe curves (dashed) resulting when D(x) is given by Eqn. 4. See text for discussion.

medium (accumulation or depletion in this region would occur when $K_d < 1$ and $K_d > 1$, respectively). This effect—described mathematically by Smith et al. (1955) and discussed by Albarède and Bottinga (1972) with reference to phenocrysts in magmas—has some appeal as an explanation for the dependence of K_{app} on V in the calcite water system: in the limit of very high V, K_{app} tends to 1 for K_d both <1 and >1. At first glance, these tendencies appear to hold for trace-element uptake in calcite. In fact, all that can be concluded from existing data is that high growth rates lead to increased K_{app} for elements with $K_d < 1$ and decreased K_{app} for elements with $K_d > 1$. The observed effects are systematic, but there is no indication of convergence to $K_{app} \sim 1$ for all elements (see Fig. 6).

The foregoing discussion, although important for clarification, is of marginal relevance to abiogenic calcite growth from aqueous solution, because diffusion of ions in water is too fast even at ambient temperatures ($D_{aq} \sim 10^9$ nm^2/s) to allow major deviations from partitioning equilibrium at any reasonable growth rate. The non–steady state equation of Smith et al. (1955) reveals, for example, that sustained growth at 1 nm/s (the highest rate shown in Fig. 6) for 1 d perturbs the near-interface concentration in the growth medium by ~10% at most relative to the initial value (this occurs when $K_d \gg 1$). For $V \leq 0.1$ nm/s, the deviation does not exceed 1%. In a real system, convective mixing of the growth medium may preclude even these very modest perturbations from equilibrium.

4. POSSIBLE IMPLICATIONS FOR OXYGEN ISOTOPES IN CALCITE

4.1. Context

The preceding section addressing the behavior Sr—which has been used as a "climate proxy" element (e.g., Schrag, 1999; Stoll and Schrag, 2001)—leads to a logical next question: Does the growth entrapment model have any bearing on the uptake of oxygen isotopes in carbonates? Given the strictly inorganic basis of the model, it would be naïve to regard surface entrapment as potentially the sole determinant of oxygen isotope ratios in skeletal carbonates, inasmuch as biologic influences are readily apparent in these materials (e.g., McConnaughey, 1989a,b). Nevertheless, in situations where the role of the organism amounts to regulating the chemical composition of the growth medium, surface entrapment effects may be superimposed upon biologic influences. If, as existing experimental data suggest, surface effects are important to the uptake of trace elements to the extent that equilibrium is rarely achieved at near-ambient temperatures, then it seems almost inevitable that stable-isotope ratios are also affected.

The purpose of this section is to explore the possible consequences of surface entrapment for oxygen isotopes in carbonates precipitated inorganically at near-ambient temperatures. At first appearances, this effort should involve a simple extension of ideas discussed earlier in this paper; there is, however, a significant complication.

In modeling oxygen isotope behavior in the calcite/H_2O system, a reasonable starting point is the equilibrium fractionation factor, α (that is, $[^{18}O/^{16}O]_{calcite}$ divided by $[^{18}O/^{16}O]_{H2O}$). One may then ask whether the growth entrapment process can produce deviations from equilibrium, and whether growth-rate dependence of measured isotope ratios might be expected. A significant obstacle to implementing the growth entrapment model is that the equilibrium fractionation factor is not known with certainty. Even the most recent studies of oxygen isotope fractionation during slow calcite precipitation from aqueous solutions (Kim and O'Neil, 1997) reveal variations in α with solution composition (concentration of bicarbonate and Ca^{2+}). The origin of these variations is uncertain: Kim and O'Neil (1997) concluded that deviations from partitioning equilibrium result during precipitation from concentrated solutions. A quite different explanation of the Kim and O'Neil data was later offered by Zeebe (1999), who deduced that $^{18}O/^{16}O$ of calcite precipitated from aqueous solution is the weighted average of the ratios of the various carbonate species (CO_2, H_2CO_3, HCO_3^-, CO_3^{2-}) present in the solution, from which the crystal is "built" (the weighted average is denoted by the symbol "S"). Zeebe arrived at this conclusion by combining two pieces of information: first, that the relative proportions of the various aqueous carbonate species depend strongly upon the pH of the solution; and, second, that the partitioning of oxygen isotopes among these species and H_2O is known (e.g., Usdowski and Hoefs, 1993). Zeebe (1999) was able to show that not only the Kim and O'Neil (1997) "inorganic" laboratory results but also the oxygen isotopic composition of foraminiferal calcite can be explained simply by varying the pH of the growth solution. In Zeebe's interpretation, changing the solution pH shifts the proportions of carbonate species in solution, thereby altering the oxygen isotope character of calcite formed from those species. The success and simplicity of this model are appealing, and it may indeed be an accurate representation of the uptake of oxygen isotopes into growing calcite. In this writer's view, however, the Zeebe treatment does not tell us about calcite/H_2O equilibrium—rather, it is an example of a mineral assuming the composition of its growth surface. There are two implicit assumptions in Zeebe's model of pH-dependent behavior: 1) that the oxygen isotope character of the surface is the same as that of the collective carbonate species; and 2) that calcite growth is sufficiently fast relative to solid-

state oxygen diffusion to perfectly capture the surface composition in the growing crystal.

Given the differences in bonding environment for oxygen in the calcite lattice as opposed to oxygen in aqueous carbonate species, isotopic fractionation must exist, at equilibrium, between the calcite lattice and the collective carbonate species. This requirement also extends to the near-surface region of calcite relative to the aqueous carbonate species *and* to the near-surface region relative to the calcite lattice (this last effect [surface/lattice fractionation] was understood—and indirectly demonstrated—by Hamza and Broecker, 1974). A corollary to the preceding statements is that there can be only one calcite/H_2O fractionation factor at a given temperature, not a range that depends on solution composition. (Strictly speaking, the equilibrium fractionation of interest is between the calcite lattice and a calcite-saturated solution containing aqueous carbonate species. However, because the vast majority of the oxygen is in H_2O molecules, this is the same, for all intents and purposes, as calcite/H_2O fractionation).

In summary, although the Zeebe model may accurately describe the behavior of oxygen isotopes in the calcite/H_2O system in the lab and in nature, it should be acknowledged that the model represents the case of complete disequilibrium in the context of the surface entrapment model: that is, total failure of solid-state diffusion to move the composition of the crystal away from that of the surface during growth (i.e., the case of Pe $\gg$ 10). How, then, can we gain insight into the other extreme (that is, complete equilibrium between the calcite lattice and water)?

4.2. Calcite/H_2O Equilibrium of Oxygen Isotopes

If isotopic equilibrium between precipitating calcite and contacting solution is not achieved in experiments at ambient conditions, the reason may be simply that diffusion of oxygen-bearing species in the near-surface of the growing crystal is too slow (slower, perhaps, than metal cations; see Fig. 7). In principle, this kinetic obstacle can be circumvented through use of an "intermediary" phase (int) that *can* be equilibrated independently with both calcite and H_2O ($\alpha_{calcite/int}/\alpha H_2O_{/int} = \alpha_{calcite/}H_2O$). Gaseous CO_2 is a suitable candidate for the intermediary phase: H_2O/CO_2 equilibrium is readily achieved because only gaseous diffusion is required; calcite/CO_2 equilibrium has been examined over a wide range of conditions, allowing accurate down-temperature extrapolation and robust theoretical modeling.

Chacko et al. (1991) examined calcite/CO_2 fractionation of oxygen isotopes at 400–800°C and 0.1 to 1.3 GPa, and showed consistency not only of their new data but also of earlier low pressure-temperature data with theoretical fractionation calculations spanning a wide range of temperature. Over the range of temperature pertinent to paleoceanography, calcite/CO_2 fractionation is given by

$$\alpha_{calcite/CO_2} = 0.98494 + 0.9866/T(K) \quad (6)$$

Expressed in similar format, the data of Brenninkmeijer et al. (1983) for H_2O/CO_2 fractionation of oxygen isotopes are described by

$$\alpha_{H_2O/CO_2} = 1.01515 - 16.29/T(K) \quad (7)$$

The relationships above lead to the following dependence of $\alpha_{calcite/H_2O}$ upon temperature:

$$\alpha_{calcite/H_2O} = 0.9666 + 18.56/T(K) \quad (8)$$

It is argued here that the fractionation factors given by Eqn. 8 represent "true" equilibrium between the *calcite lattice* and H_2O. Some uncertainty in the accuracy of the relationship arises from the fact that Eqn. 6 is based upon theoretical calculations (see Chacko et al., 1991). These calculations are consistent with experimental data, but most of the data pertain to relatively high pressure-temperature conditions, so their relevance is not indisputable (note, on the positive side, that the calculations of Rosenbaum, 1997, reveal little difference in the reduced partition function ratios for gaseous and supercritical CO_2). This disclaimer aside, Eqn. 8 gives almost exactly the same fractionation factors and temperature dependence as the relationship favored by Friedman and O'Neil (1977) over the temperature range of interest in this paper. Figure 11 is a comparison of predicted and measured calcite/H_2O fractionation behavior for oxygen isotopes from several different studies. Interestingly, the values calculated using the "intermediary" phase approach taken here are bracketed by the determinations of Kim and O'Neil (1997). In relation to Zeebe's (1999) interpreted pH dependence, Eqn. 8 gives values coincident with a pH of ~7–7.5 (see Fig. 11b). Again, however, the present writer's belief is that there can be only one calcite/H_2O fractionation factor that represents true equilibrium at a given temperature, independent of pH for all intents and purposes.

4.3. Possible Growth Entrapment Effects on Oxygen Isotope Ratios

Armed with a tentative description of "true" lattice/fluid partitioning equilibrium for calcite/H_2O (Eqn. 8) and a starting point from which to characterize the surface composition (that of Zeebe, 1999), numerical simulations of the growth entrapment process can be run for oxygen. Unfortunately, all of the uncertainties encountered in modeling behavior of cations (i.e., in l, D_S and m) also apply to oxygen. No information whatsoever exists on oxygen diffusion in the near-surface region of calcite, so the greatest uncertainty in any model incorporating actual dimensions and rates lies in knowledge of D_S. As a possible basis for comparison with cation behavior, published data on oxygen diffusion in the calcite lattice are included in Figure 7; however, it is cautioned that even the relative positions of the various diffusivities on the Arrhenius plot are not necessarily preserved to low temperature, nor from one material (the "normal" calcite lattice) to another (the near-surface region). The lowest-temperature lattice diffusion results encourage the speculation that oxygen diffusion is much slower that that of small, divalent cations (see Fig. 7). This seems reasonable in the respect that oxygen may diffuse as a relatively large molecule or ion.

The possible differences between the oxygen isotope ratio of the near-surface region and that of the equilibrium crystal lattice can be appreciated with reference to Figure 12, which is adapted from Zeebe's (1999) discussion of pH dependence (see his fig. 4) at constant temperature (19°C). Figure 12a shows the

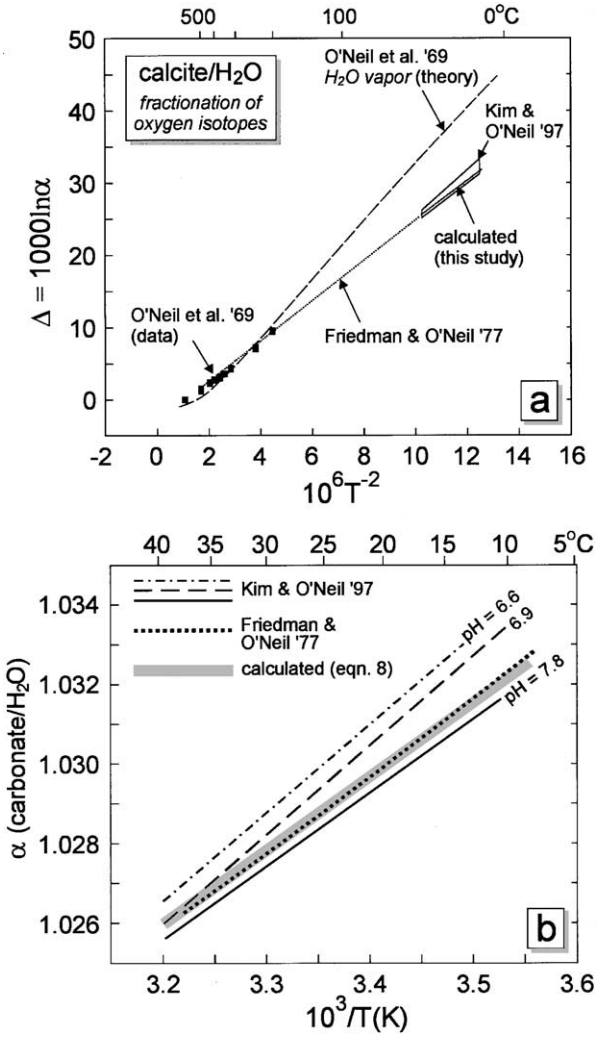

Fig. 11. Summary of data and models for oxygen isotope fractionation between calcite and H_2O. The diagram in (a) covers the full range of temperature over which data are available, and shows the broad consistency between the data of O'Neil and coworkers (O'Neil et al., 1969; Friedman and O'Neil, 1977; Kim and O'Neil, 1997) and values calculated by dividing $\alpha_{calcite/CO2}$ (from Chacko et al., 1991) by $\alpha_{H2O/CO2}$ (from Brenninkmeijer et al., 1983). In (b) the calculated values are compared more closely at temperatures of interest in the present study. The indicated pH values represent Zeebe's (1999) interpretation of the data of Kim and O'Neil (1997). See text for discussion.

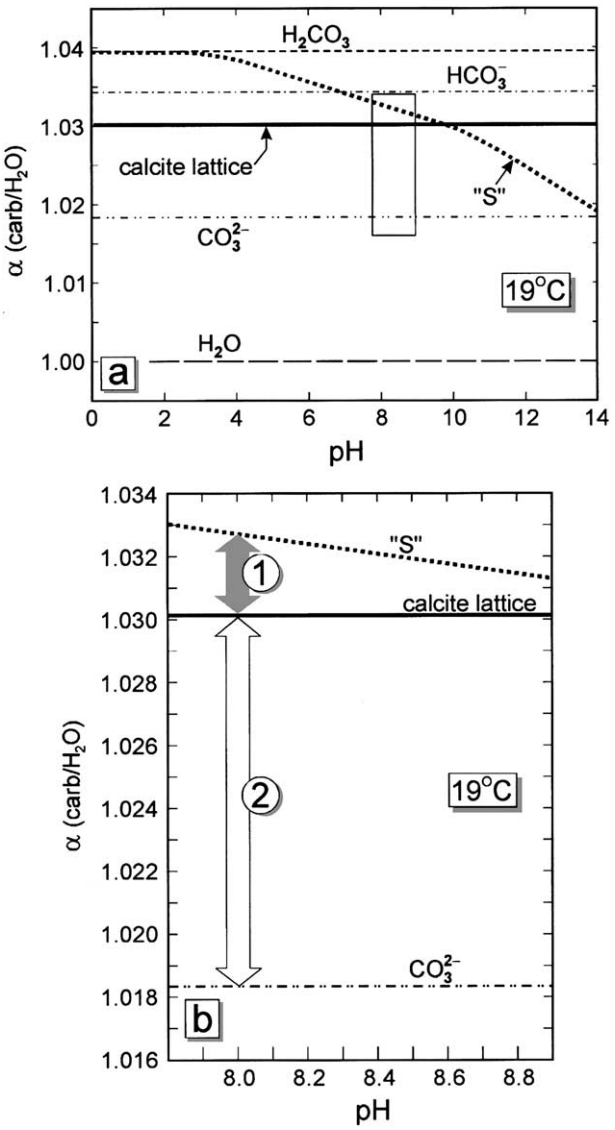

Fig. 12. Oxygen isotope fractionation among calcite, aqueous carbonate species and H_2O as a function of pH at 19°C (modified from Zeebe, 1999). In (a) the curve "S" represents the weighted average of the aqueous carbonate species present at a given pH. The line labeled "calcite lattice" at $\alpha \sim 1.03$ is from Eqn. 8. The area in the rectangular box is enlarged in (b) to show the differences among the fractionation factors for the calcite lattice, "S," and aqueous CO_3^{2-} relative to H_2O over the pH range of interest in paleoceanography. The shaded arrow labeled "1" emphasizes the difference between oxygen isotopes in the calcite lattice and in "S" (one possible model for the calcite surface) at normal seawater pH. The arrow labeled "2" is the difference between the calcite lattice and aqueous CO_3^{2-} (another isotopic candidate for the calcite surface). Calcite growth would tend to "capture" the isotopic character of the surface as illustrated in Figure 13.

pH-independent isotopic character of the various aqueous carbonate species in equilibrium with H_2O, but emphasizes that as the proportions of these species in the solution change with increasing pH, the weighted average "S" defines a curve with negative slope.

In the discussion below, two alternative assumptions are made regarding oxygen isotopes in the near-surface. In the first case—the "Zeebe surface" model—the curve "S" in Figure 12 is taken as representing the isotopic composition of the calcite surface during growth (see section 4.1). For simulation purposes, then, the key question concerns the degree to which "S" deviates from the true equilibrium value for isotopic fractionation between the normal calcite lattice and H_2O. According to Eqn. 8, $\alpha_{calcite/H2O}$ is 1.0302. In the pH range of interest in this paper, "S" always lies above the calcite lattice equilibrium value (see Fig. 12b), so at equilibrium the surface is enriched in ^{18}O relative to the calcite lattice, just as in the case of Sr (see section 3.3). As a calcite crystal grows, diffusion in the near-surface region will attempt to convert the surface value ($\sim$1.033 at pH$\sim$8) to the equilibrium lattice value ($\sim$1.0302); this difference is indicated by the arrow labeled "1" in Figure 12b. The competition between growth and diffusion—the essence of the growth entrapment model—requires the existence of a critical range of V/D_S in which the ^{18}O concentration of the

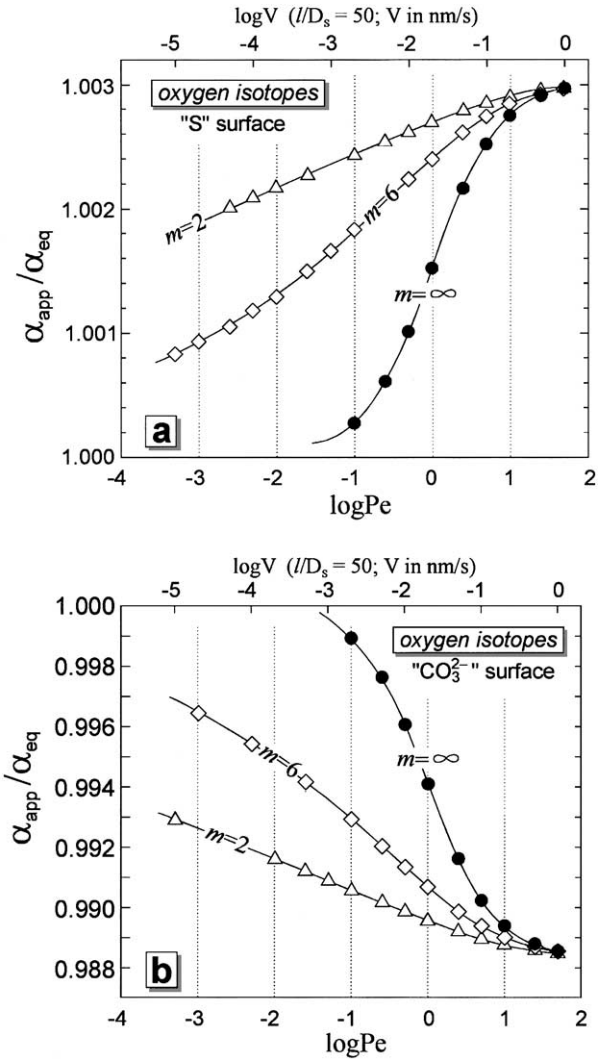

Fig. 13. Entrapment efficiency of disequilibrium oxygen isotope ratios as a function of logPe. The apparent equilibrium fractionation factor, α_{app}, is that recorded by the growing crystal; α_{eq} is the true equilibrium value. In (a), $^{18}O/^{16}O$ of the surface is assumed to be the same as "S"; in (b) it is assumed to be aqueous CO_3^{2-}. See text and Figure 12.

resulting calcite crystal depends on growth rate. Because "S" lies above the "calcite lattice" line in Figure 12b, the Zeebe-surface model results in a calcite ^{18}O level in excess of the lattice equilibrium value at high growth rates. This amounts to growth entrapment of ^{18}O.

Figure 13a summarizes oxygen isotope model results at pH = 8 for a range of growth rate and diffusion conditions, given a surface composition equivalent to S. Deviations from oxygen isotope equilibrium between the calcite lattice and H_2O are expressed as the apparent fractionation factor (α_{app}) divided by the equilibrium value (α_{eq}). Because the difference between the assumed "surface" value, S, and the equilibrium lattice value given by Eqn. 8 is ~3‰, this is the maximum deviation from equilibrium that is achievable at high growth rates. The overall implication of these calculations is that—all else being equal—fast growth pushes the oxygen isotopic character of calcite toward heavier values. Interestingly, the implied maximum spread in $\delta^{18}O$ of ~3‰ that could be produced by a marked change in growth rate is actually larger than that resulting from a change in pH from 7.8 to 8.9 in Zeebe's (1999) model (see Fig. 12b). A potentially problematic aspect of this result is that it suggests a dependence of $\delta^{18}O$ upon calcite growth rate opposite to that actually observed in nature (e.g., Adkins et al., 2003).

The alternative "end-member" assumption made in the modeling was that the oxygen isotope character of the calcite surface is similar to that of aqueous CO_3^{2-} ions. In some respects, this is considered to be a more realistic starting point. Recent in situ characterizations of the calcite/H_2O interface (Stipp, 1999; Fenter et al., 2000) are consistent with the surface complexation model of van Cappellen et al. (1993) in revealing CO_3 groups and Ca atoms in the outermost monolayer, with hydroxyls in the contacting solution bonded specifically to Ca. In terms of the local bonding environment for oxygen, the surface would thus be quite different from that in a mixture of aqueous carbonate ions (CO_2, H_2CO_3, HCO_3^-, CO_3^{2-}). Closer resemblance might be expected to aqueous CO_3^{2-} ions specifically, or to a structural intermediate between CO_3^{2-} and the calcite lattice. In evaluating this model against the Zeebe surface assumption used previously, it may be significant that Fenter et al. (2000) observed little or no difference in atomic structure of the calcite/H_2O interface at pH = 8.3 relative to pH = 12.1. Lack of pH sensitivity of surface structure may argue against S as representative of the calcite surface, because S = f(pH) (Fig. 12).

It is assumed for the remaining simulations that the calcite surface is isotopically similar to aqueous CO_3^{2-} ions. In this case, the isotopic difference between the calcite lattice and the surface is indicated by the arrow labeled "2" in Figure 12b. The difference may not be as extreme as the 12‰ shown on the diagram, but as long as the fractionation factor for the surface lies below that for the calcite lattice, the qualitative implications for the numerical growth simulations are the same.

The results of simulations assuming a "CO_3^{2-}" surface are shown in Figure 13b. the curves for m = 2, 6 and ∞ can be thought of as "growth exclusion" curves for ^{18}O in the sense that isotopically lighter calcite is favored at higher growth rates. As noted previously, the 12‰ total range may be unrealistically large, but it appears possible to reproduce the negative correlation between growth rate and $\delta^{18}O$ of some natural skeletal carbonates (Adkins et al., 2003).

The details of the foregoing conclusions clearly hinge not only upon the validity of the assumed surface composition but also upon the accuracy of the calculated calcite/H_2O fractionation factor for oxygen isotopes. However, the overall significance of the finding does not: the only assumption that is crucial to the ability of growth entrapment/exclusion to affect oxygen isotope ratios of calcite is that $\alpha_{calcite/H2O}$ differ from $\alpha_{surface/H2O}$.

No attempt was made to model C isotopes because the assumptions needed to do so seem even less certain than those made for oxygen. It is noted, however, that carbon diffuses more slowly than any other component in the normal calcite lattice at T < 600°C (Fig. 7); if this mobility ranking also applies to the near-surface region of calcite at ~20°C, then the C isotope ratio of calcite precipitated from water probably does not reflect true lattice/H_2O equilibrium.

In closing this section, it should be noted that diffusion

processes involving isotopes cannot always be treated in the same manner as those involving trace elements. Both oxygen and carbon are major components of calcite, and their isotope sums ($^{18}O + {}^{16}O$ and $^{13}C + {}^{12}C$) are fixed by crystal stoichiometry. Any diffusion process must involve interdiffusion of the two isotopes, and it is not strictly correct to regard the ratio (e.g.,$^{18}O/^{16}O$) as the "diffusant," as was implicitly done here. However, because ^{16}O constitutes the vast majority of all oxygen, there is essentially no inaccuracy introduced in doing so (see, e.g., section 4.1 of Watson and Cherniak, 1997). It should be noted, also, that because the extent of growth entrapment (exclusion) depends in part on the mobility of ions in the near-surface of the crystal, and because the diffusivities (D_S) of the light and heavy isotopes are expected to differ slightly, diffusive fractionation in the near-surface layer is not inconceivable. This possibility was discussed by Turner (1982), but new information about diffusive fractionation in condensed phases has become available since his paper was published. Recent studies of Ca-, Ge- and Li-isotope fractionation by diffusion in silicate melts (Richter et al., 1999, 2003) reveal smaller differences than are predicted by the kinetic theory of gases, which was used by Turner (1982) to evaluate the relative diffusivities of carbon isotopes. The magnitude of the mass effect on diffusion may be immaterial anyway, because total O and total C are fixed by crystal stoichiometry—which means that the two isotopes of each element cannot diffuse independently. In such a case, diffusive exchange is governed by the slower isotope. Lastly, even if the stoichiometric constraint is relaxed in the near-surface region, diffusive fractionation of isotopes is most effective when the two interdiffusing reservoirs are substantially different with respect to concentration of the element of interest. The calcite lattice and the near-surface region are virtually identical in this respect.

Recent simulations involving numerical solution of diffusion-reaction equations (Zeebe et al., 1999) show that differences in carbon isotope uptake in foraminiferal shells can result from processes occurring in the surrounding growth medium. Any contribution of growth entrapment processes to C isotope fractionation during shell growth would be additive to such effects.

5. CONCLUDING REMARKS

There are two broad conclusions of this study that may bear on the trace element and stable isotope composition of natural calcites. The first is that the growth entrapment model is consistent with observed variations in trace-element uptake with growth rate under abiogenic conditions, both in nature and in the lab. This conclusion is phrased in a conservative way because, given the number of adjustable parameters, the model results do not prove cause and effect. However, the principles embodied in the model are believed to be substantially correct, in essence if not in detail. The single key premise is that there are differences in atomic structure, chemical composition, and atom mobility between the "interior" lattice of a calcite crystal and its near-surface region (the latter taken to mean the outermost monolayers of the crystal and the "laterally averaged," stepped growth surface itself). From this premise follows the requirement that, as growth occurs, the structure and composition of the former surface must adjust to that of the normal calcite lattice in order for equilibrium to be maintained. The remaining assumptions involve choices of the manner in which to describe length scales and rates of molecular reorganization of the near-surface region during growth. These are details of the modeling approach that affect the results only qualitatively.

To give credit where it is due, it is clear that the concept of growth entrapment was grasped decades ago by Kinsman and Holland (1969). The present contribution, following that of Watson and Liang (1995) and Watson (1996), was to formalize the model and investigate hypothetical growth/diffusion scenarios. Qualitative consistency of the growth-entrapment model with observed behavior of Sr in calcite was first confirmed by Stoll et al. (2002), using "version 1.0" of the model, in which $D \neq f(x)$ (i.e., $m = \infty$). Any added value of the present contribution stems from the realization that D must vary with distance from the crystal surface (which changes the behavior of the system substantially), and that near-surface depletion of trace elements is just as plausible as near-surface enrichment. The fact that the present model easily accommodates negative as well as positive dependencies of apparent partition coefficients upon growth rate may be a significant selling point: it is not clear that interface-reaction control could produce the same result.

The second general conclusion of this paper is that stable isotope ratios may be affected by growth rate through the surface entrapment process. Example simulations are used to show that $^{18}O/^{16}O$ of calcite may show a positive or negative correlation with growth rate at constant temperature over some range of V/D_S, depending upon the assumed equilibrium isotopic character of the surface. It is argued here that high growth rates probably lead to lower $^{18}O/^{16}O$ values.

Because most of the parameters of the surface entrapment model are poorly constrained, it would be naïve to regard the results of this study as an accurate description of trace-element and isotope behavior in natural calcite under any circumstances. The hope is that the model will provide a stimulus and framework for further discussion of "inorganic" kinetic disequilibrium effects, as well as incentive for additional measurements (of, for example, diffusion in the near-surface region). Even in the absence of biologic mediation, the number of factors potentially affecting isotope and elemental ratios in natural calcites is large ("thermodynamic" temperature effects on partitioning may, for example, superimpose upon the kinetic effects related to growth rate and diffusion—both of which are temperature-dependent in themselves). The best strategy in approaching this dauntingly complex problem is to identify the possible factors and assess the likely magnitude of their influence on a case-by-case basis. The potential role of surface-related kinetic phenomena appears to remain significant.

Acknowledgments—The following individuals generously provided their time and insight into various aspects of calcite growth, surface chemistry and oxygen isotope behavior: Jun Abrajano, Bob Clayton, Tom Chacko, Trish Dove, Mike Hochella, Yan Liang, Frank Richter, Susan Stipp, Heather Stoll and Laura Wasylenki (any omissions and misconceptions in the paper, however, are those of the author). Don Drew of RPI's Math Department advised on the topic of lateral averaging. Anne Cohen provided the encouragement to revisit the surface enrichment model in the context of carbonate growth in seawater, and Neil Sturchio and Jess Adkins provided insightful official reviews of the manuscript. The research was supported by the National Science Foundation under grant EAR-9804794.

Associate editor: R. H. Byrne

REFERENCES

Adkins J. F., Boyle E. A., Curry W. B., and Lutringer A. (2003) Stable isotopes in deep-sea corals and a new mechanism for "vital effects." *Geochim. Cosmochim. Acta* **67,** 1129–1143.

Ahmad N. A., Wheeler A. A., Boettinger W. J., and McFadden G. B. (1998) Solute trapping and solute drag in a phase-field model for rapid solidification. *Phys. Rev. E* **58,** 3436–3450.

Albarède F. and Bottinga Y. (1972) Kinetic disequilibrium in trace element partitioning between phenocrysts and host lava. *Geochim. Cosmochim. Acta* **36,** 141–156.

Aziz M. J. (1982) Model for solute redistribution during rapid solidification. *J. Appl. Phys.* **53,** 1158–1168.

Aziz M. J. (1996) Interface attachment kinetics in alloy solidification. *Metall. Mat. Trans. A* **27,** 671–685.

Bedzyk M. J. and Cheng L. (2002) X-ray standing wave studies of minerals and mineral surfaces: Principles and applications. In *Reviews in Mineralogy and Geochemistry* **49** (eds. P. A. Fenter, M. L. Rivers, N. C. Sturchio, and S. R. Sutton), pp. 221–266. Mineralogical Society of America.

Brenninkmeijer C. A. M., Kraft P., and Mook W. G. (1983) Oxygen isotope fractionation between CO_2 and H_2O. *Chem. Geol. (Isot. Geosc. Sect.)* **1,** 181–190.

Chacko T., Mayeda T. K., Clayton R. N., and Goldsmith J. R. (1991) Oxygen and carbon isotope fractionations between CO_2 and calcite. *Geochim. Cosmochim. Acta* **55,** 2867–2882.

Cherniak D. J. (1997) An experimental study of strontium and lead diffusion in calcite, and implications for carbonate diagenesis and metamorphism. *Geochim. Cosmochim. Acta* **61,** 4173–4179.

Crank J. (1975) *The Mathematics of Diffusion* 2nd ed. Oxford University Press.

Davis J. A., Fuller C. C., and Cook A. D. (1987) A model for trace metal sorption processes at the calcite surface: Adsorption of Cd^{2+} and subsequent solid-solution formation. *Geochim. Cosmochim. Acta* **51,** 1477–1490.

Drew D. A. and Passman S. L. (1998) *Theory of Multicomponent Fluids*. Springer.

Dromgoole E. L. and Walter L. M. (1990) Iron and manganese incorporation into calcite: Effects of growth kinetics, temperature, and solution chemistry. *Chem. Geol.* **81,** 311–336.

Farver J. R. (1994) Oxygen self-diffusion in calcite: Dependence on temperature and water fugacity. *Earth Planet. Sci. Lett.* **121,** 575–587.

Farver J. R. and Yund R. A. (1996) Volume and grain boundary diffusion of calcium in natural and hot-pressed calcite aggregates. *Contrib. Mineral. Petrol.* **123,** 77–91.

Fenter P., Geissbühler P., DiMasi E., Srajer G., Sorensen L. B., and Sturchio N. C. (2000) Surface speciation of calcite observed by in situ high-resolution X-ray reflectivity. *Geochim. Cosmochim. Acta* **64,** 1221–1228.

Fisler D. K. and Cygan R. T. (1999) Diffusion of Ca and Mg in calcite. *Am. Mineral.* **84,** 1392–1399.

Friedman I. and O'Neil J. R. (1977) Compilation of stable isotope fractionation factors of geochemical interest. Prof. Paper 440-KK. USGS.

Hamza M. S. and Broecker W. S. (1974) Surface effect on the isotopic fractionation between CO_2 and some carbonate minerals. *Geochim. Cosmochim. Acta* **38,** 669–681.

Hoffmann U. and Stipp S. L. S. (2001) The behavior of Ni^{2+} on calcite surfaces. *Geochim. Cosmochim. Acta* **65,** 4131–4139.

Kent A. J. R., Hutcheon I. D., Ryerson F. J., and Phinney D. L. (2001) The temperature of formation of carbonate in Martian meteorite ALH84001: Constraints from cation diffusion. *Geochim. Cosmochim. Acta* **65,** 311–321.

Kim S.-T. and O'Neil J. R. (1997) Equilibrum and nonequilibrium oxygen isotope effects in synthetic carbonates. *Geochim. Cosmochim. Acta* **61,** 3461–3475.

Kinsman D. J. J. and Holland H. D. (1969) The co-precipitation of cations with $CaCO_3$—IV. The co-precipitation of Sr^{2+} with aragonite between 16° and 96°C. *Geochim. Cosmochim. Acta* **33,** 4–17.

Kronenberg A. K., Yund R. A., and Giletti B. J. (1984) Carbon and oxygen diffusion in calcite: Effects of Mn content and P_{H2O}. *Phys. Chem. Minerals* **11,** 102–111.

Labotka T. C., Cole D. R., and Riciputi L. R. (2000) Diffusion of C and O in calcite at 100 MPa. *Am. Mineral.* **85,** 488–494.

Lorens R. B. (1981) Sr, Cd, Mn and Co distribution coefficients in calcite as a function of calcite precipitation rate. *Geochim. Cosmochim. Acta* **45,** 553–561.

McConnaughey T. (1989a) ^{13}C and ^{18}O isotopic disequilibrium in biological carbonates: I. Patterns. *Geochim. Cosmochim. Acta* **53,** 151–162.

McConnaughey T. (1989b) ^{13}C and ^{18}O isotopic disequilibrium in biological carbonates: II. In vitro simulation of kinetic isotope effects. *Geochim. Cosmochim. Acta* **53,** 163–171.

O'Neil J. R., Clayton R. N., and Mayeda T. K. (1969) Oxygen isotope fractionation in divalent metal carbonates. *J. Chem. Phys.* **51,** 5547–5558.

Paquette J. and Reeder R. J. (1995) Relationship between surface structure, growth mechanism, and trace element incorporation in calcite. *Geochim. Cosmochim. Acta* **59,** 735–749.

Reeder R. J. (1996) Interaction of divalent cobalt, zinc, cadmium, and barium with the calcite surface during layer growth. *Geochim. Cosmochim. Acta* **60,** 1543–1552.

Reeder R. J. and Paquette J. (1989) Sector zoning in natural and synthetic calcites. *Sediment. Geol.* **65,** 239–247.

Reeder R. J., Elzinga E. J., and Rouff A. (2002) Coordination of some metals sorbed at the calcite-water interface (abstract). *Geochim. Cosmochim. Acta* **66,** A628.

Richter F. M., Liang Y., and Davis A. M. (1999) Isotope fractionation by diffusion in molten oxides. *Geochim. Cosmochim. Acta* **63,** 2853–2861.

Richter F. M., Davis A. M., DePaolo D. J., and Watson E. B. (2003) Isotope fractionation by chemical diffusion between molten basalt and rhyolite. *Geochim. Cosmochim. Acta* **67,** 3905–3923.

Rohl A. L., Wright K., and Gale J. D. (2003) Evidence from surface phonons for the (2×1) reconstruction of the $(10\bar{1}4)$ surface of calcite from computer simulation. *Am. Mineral.* **88,** 921–925.

Rosenbaum J. M. (1997) Gaseous, liquid, and supercritical fluid H_2O and CO_2: Oxygen isotope fractionation behavior. *Geochim. Cosmochim. Acta* **61,** 4993–5003.

Schrag D. P. (1999) Rapid analysis of high-precision Sr/Ca ratios in corals and other marine carbonates. *Paleoceanography* **14,** 97–102.

Smith V. G., Tiller W. A., and Rutter J. W. (1955) A mathematical analysis of solute redistribution during solidification. *Can. J. Phys.* **33,** 723–744.

Stipp S. L. S. (1998) Surface analytical techniques applied to calcite: Evidence of solid-state diffusion and implications for isotope methods. *Paleogeogr. Paleoclimatol. Paleoecol.* **140,** 441–457 3.

Stipp S. L. S. (1999) Toward a conceptual model of the calcite surface: Hydration, hydrolysis, and surface potential. *Geochim. Cosmochim. Acta* **63,** 3121–3131.

Stipp S. L., Hochella M. F., Parks G. A., and Leckie J. O. (1992) Cd^{2+} uptake by calcite, solid-state diffusion, and the formation of solid-solution: Interface processes observed with near-surface sensitive techniques (XPS, LEED, and AES). *Geochim. Cosmochim. Acta* **56,** 1941–1954.

Stipp S. L. S., Konnerup-Madsen J., Franzreb K., Kulik A., and Mathieu H. J. (1998) Sponaneous movement of ions through calcite at standard temperature and pressure. *Nature* **396,** 356–359.

Stoll H. M. and Schrag D. P. (2001) Sr/Ca variations in Cretaceous carbonates: Relation to productivity and sea level changes. *Paleogeogr. Paleoclimatol. Paleoecol.* **168,** 311–336.

Stoll H. M., Rosenthal Y., and Falkowski P. (2002) Climate proxies from Sr/Ca of coccolith calcite: Calibrations from continuous culture of. *Emiliania huxleyi*. *Geochim. Cosmochim. Acta* **66,** 927–936.

Teng H. H., Dove P. M., and De Yoreo J. J. (2000) Kinetics of calcite growth: Surface processes and relationships to macroscopic rate laws. *Geochim. Cosmochim. Acta* **64,** 2255–2266.

Tesoriero A. J. and Pankow J. F. (1996) Solid solution partitioning of Sr^{2+}, Ba^{2+}, and Cd^{2+} to calcite. *Geochim. Cosmochim. Acta* **60,** 1053–1063.

Tiller W. A. (1991) *The Science of Crystallization: Microscopic Interfacial Phenomena*. Cambridge University Press.

Tiller W. A. and Ahn K.-S. (1980) Interface field effects on solute redistribution during crystallization. *J. Crystal Growth* **49,** 483–501.

Turner J. V. (1982) Kinetic fractionation of carbon-13 during calcium carbonate precipitation. *Geochim. Cosmochim. Acta* **46,** 1183–1191.

van Cappellen P., Charlet L., Stumm W., and Wersin P. (1993) A surface complexion model of the carbonate mineral-aqueous solution interface. *Geochim. Cosmochim. Acta* **57,** 3505–3518.

Usdowski E. and Hoefs J. (1993) Oxygen isotope exchange between carbonic acid, bicarbonate, carbonate, and water: A re-examination the data of McCrea (1950) and an expression for the overall partitioning of oxygen isotopes between the carbonate species and water. *Geochim. Cosmochim. Acta* **57,** 3815–3818.

Watson E. B. (1996) Surface enrichment and trace-element uptake during crystal growth. *Geochim. Cosmochim. Acta* **60,** 5013–5020.

Watson E. B. and Liang Y. (1995) A simple model for sector zoning in slowly grown crystals: Implications for growth rate and lattice diffusion, with emphasis on accessory minerals in crustal rocks. *Am. Mineral.* **80,** 1179–1187.

Watson E. B. and Cherniak D. J. (1997) Oxygen diffusion in zircon. *Earth Planet. Sci. Lett.* **148,** 527–544.

Zeebe R. E. (1999) An explanation of the effect of seawater carbonate concentration on foraminiferal oxygen isotopes. *Geochim. Cosmochim. Acta* **63,** 2001–2007.

Zeebe R. E., Bijma J., and Wolf-Gladrow D. A. (1999) A diffusion-reaction model of carbon isotope fractionation in foraminifera. *Mar. Chem.* **64,** 199–227.